

Autonomous Robotic Radio Source Localization via a Novel Gaussian Mixture Filtering Approach

Sukkeun Kim 

Faculty of Engineering and Applied Sciences
Cranfield University
Cranfield, UK

Jet Propulsion Laboratory
California Institute of Technology
Pasadena, USA

Sangwoo Moon 

Jet Propulsion Laboratory
California Institute of Technology
Pasadena, USA

Ivan Petrunin 

Faculty of Engineering and Applied Sciences
Cranfield University
Cranfield, UK

Hyo-Sang Shin 

Faculty of Engineering and Applied Sciences
Cranfield University
Cranfield, UK

Cho Chun Shik Graduate School of Mobility
Korea Advanced Institute of Science and Technology
Daejeon, Republic of Korea

Shehryar Khattak 

Jet Propulsion Laboratory
California Institute of Technology
Pasadena, USA

Abstract—This study proposes a new Gaussian Mixture Filter (GMF) to improve the estimation performance for the autonomous robotic radio signal source search and localization problem in unknown environments. The proposed filter is first tested with a benchmark numerical problem to validate the performance with other state-of-the-practice approaches such as Particle Filter (PF) and Particle Gaussian Mixture (PGM) filters. Then the proposed approach is tested and compared against PF and PGM filters in real-world robotic field experiments to validate its impact for real-world applications. The considered real-world scenarios have partial observability with the range-only measurement and uncertainty with the measurement model. The results show that the proposed filter can handle this partial observability effectively whilst showing improved performance compared to PF, reducing the computation requirements while demonstrating improved robustness over compared techniques.

Index Terms—Radio signal source search, Bayesian estimation, Gaussian mixture filter, particle filter.

I. INTRODUCTION

Autonomous robotic radio signal source search and localization is a problem in which the robot actively searches for the radio signal source in an unknown environment. Denniston *et al.* [1] proposed a graph model for robotic radio signal source search which can be scaled to a large number of measurements. Azuma *et al.* [2] proposed a controller for the signal source search in the completely unknown space based on the simultaneous-perturbation stochastic approximation algorithm. Li *et al.* [3] proposed and tested cooperative multi-robot source search problem with gradient descent and

The research was carried out at the Jet Propulsion Laboratory, California Institute of Technology, under a contract with the National Aeronautics and Space Administration (80NM0018D0004).

©2025. California Institute of Technology. All rights reserved.

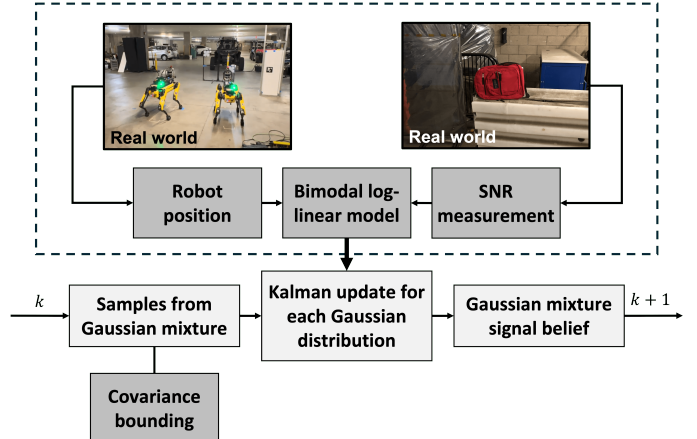


Fig. 1: **Overview of approach.** At the given time instance, the filter takes the real-world robot position and SNR measurement as input to update the filter by calculating the predicted signal strength with bimodal log-linear model. The filter then outputs Gaussian mixture signal belief.

Turgemen and Werner [4] proposed Multiple Extrema Search Algorithm (MESA) for source search with multiple agents.

However, partial observability is one of the biggest issues in the robotic radio signal source search problem due to either no prior knowledge regarding the search environment or due to the limitation of the sensor [5], [6]. This issue can be compensated by the incremental exploration of the unknown environment by the robot; however, the radio signal search problem can become intractable if the robot conducts a

naive exploration of the unknown space without leveraging the radio signal source information to guide its search even if the environment size is within the robots operational capabilities. To alleviate this issue, multiple estimation algorithms were considered for the autonomous robotic signal source search. Clark *et al.* [7] proposed Propagation Environment Modelling and Learning (PropEm-L) to enhance the radio signal by extracting Line-of-Sight (LOS) information. However, this requires an understanding of maps and geometry. To remove these constraints and apply it to real-time applications, estimation filters such as Extended Kalman Filter (EKF) or Particle Filter (PF) [8], [9], [10] are considered. However, PFs suffer from the curse of dimensionality and the performance of the PF can be significantly degraded if the diversity of the particles is lost, typically referred to as the particle degeneracy and impoverishment problem [11]. To alleviate these issues, Bayes filters with Gaussian Mixture Model (GMM) have been proposed. However, Gaussian Sum Filter (GSF) [12], which is the original idea of Gaussian Mixture Filter (GMF), and its variants have an issue of covariance collapse in complex scenarios. Another approach, the Particle Gaussian Mixture (PGM) filter and its variant [13], [14], [15] resolved this issue but required high computation. Furthermore, the PGM filters are not able to approximate the ring-shaped signal belief in the range-only measurement scenario which is the case for the considered radio source localization problem. In this study, we propose a novel GMF for the autonomous robotic radio signal source search and localization problem. The proposed filter considers each particle as a Gaussian component to approximate the posterior distribution and is equipped with Matrix Inequality (MI) bounding to set the upper limit of the covariance of each component and uses a scaled sample covariance for resampling. These points distinguish the proposed filter from previous ones. Then it was compared with the state-of-practice PF and PGM filters. The overview of the proposed approach is shown in Fig. 1. The main contributions of this study are listed as follows:

- 1) A new Gaussian Mixture Filter (GMF) with MI bounding and scaled sample covariance is proposed for autonomous robotic radio signal source search and localization in unknown environments.
- 2) The proposed filter is validated using a numerical simulation and tested in real-world robotic scenarios using a team of legged NeBula-Spot robots.
- 3) Comparisons with multiple state-of-the-art nonlinear filters are conducted to provide a comprehensive analysis.

The rest of this paper is composed as follows: Section II briefly introduces the PF and PGM filters. Section III introduces the proposed GMF approach and Section IV presents the simulation result of the proposed method on a benchmark numerical example. Section V demonstrates the real-world application of the proposed approach for conducting autonomous robotic radio signal source search experiments in complex unknown environments, followed by the discussion. Finally, we conclude this study with future work in Section VI.

II. PRELIMINARIES

A. Particle Filter

PF is a sample-based recursive Bayesian estimation in which the samples approximate the posterior distribution of the state. The general form of the Probability Density Function (PDF) of the recursive Bayesian estimation can be calculated as follows:

$$p(\mathbf{x}_k | \mathbf{z}_{1:k}) = \frac{p(\mathbf{z}_k | \mathbf{x}_k)p(\mathbf{x}_k | \mathbf{z}_{1:k-1})}{\int p(\mathbf{z}_k | \mathbf{x}_k)p(\mathbf{x}_k | \mathbf{z}_{1:k-1})d\mathbf{x}_k}, \quad (1)$$

where the subscript $k = 1, 2, 3 \dots$ implies the time instance, \mathbf{x}_k is the state vector and \mathbf{z}_k is the measurement vector. However, an analytical solution of Eq. (1) is not obtainable for most cases. PF approximates Eq. (1) with samples and Dirac delta function as follows:

$$p(\mathbf{x}_k | \mathbf{z}_{1:k}) \simeq \sum_{i=1}^{N_p} w_i \delta(\mathbf{x}_k - \mathbf{x}_k^i), \quad (2)$$

where N_p is the total number of particles, w_i is the weight of i^{th} particle which sums up to 1, $\delta(\cdot)$ is the Dirac delta function and \mathbf{x}_k^i is the belief state of the i^{th} particle. A simple Sequential Importance Resampling (SIR) is utilized for comparison in this study.

B. Particle Gaussian Mixture Filter

PGM filters are the extension of PF bringing the GMM into the PF to improve the performance of PF. PGM filters were originally proposed to overcome the particle degeneracy issue by approximating the PDF of the state as a GMM. In order to approximate the PDF with GMM, the particles are first clustered with modified K-means clustering [13], [14] or Density-based Spatial Clustering of Applications with Noise (DBSCAN) [15], and each cluster is considered as a Gaussian component. A total number of mixture in the GMM is N_m and the GMM can be calculated as follows:

$$GMM(\mathbf{x}) = \sum_{n=1}^{N_m} w_n \mathcal{N}(\boldsymbol{\mu}_n, \boldsymbol{\sigma}_n^2), \quad (3)$$

where w_n is the weight of the n^{th} Gaussian component which sums up to 1 and $\boldsymbol{\mu}_n$ and $\boldsymbol{\sigma}_n^2$ are mean and variance of n^{th} Gaussian component, respectively. The new particles for the next time step are sampled from the GMM in Eq. (3) during the resampling step. In this study, we compare the PGM filter with DBSCAN (PGM-DS) and the PGM filter with DBSCAN and Unscented Transform (UT) (PGM-DU). Further details about these filters can be found in Table I and in [15].

III. GAUSSIAN MIXTURE FILTER

The proposed GMF and PGM filters both assume the GMM for their PDF of the state but differ in the approach for the GMM construction. Instead of clustering the particles to form the Gaussian distribution and reconstructing the GMM with these Gaussian components, the proposed GMF considers each particle as a Gaussian distribution. Next, each Gaussian component is propagated directly with nonlinear dynamics and

TABLE I: Comparison of PF, PGM filters and proposed filter.

Step	PF	PGM filters	Proposed
Initialization	Random samples from Gaussian distribution. No assumed covariance.	Random samples from Gaussian distribution. No assumed covariance.	Random samples from Gaussian distribution. Assumed covariance with bandwidth parameter.
Time propagation	Using dynamics directly. No propagation of covariance.	Using dynamics directly. No propagation of covariance.	Using dynamics directly. Covariance propagation with Jacobian.
Clustering	-	Particle clustering for update. Sample covariance of each cluster.	-
MI bounding	-	-	Covariance bounding with scaled sample covariance.
Measurement update	Weight update with measurement likelihood.	Update like EKF with sample covariance (but no covariance update). Weight update with measurement likelihood.	Update like EKF with covariance from the previous step (with covariance update). Weight update with measurement likelihood.
Resampling	Resampling with weight and number of effective particles.	Resample from GMM.	Resample from GMM and reset the covariance with scaled sample covariance.

updated in the same manner as it is done in an EKF. However, the uncertainty can be increased after the time propagation and this causes the increase of the covariance of each particle. The increment of individual covariance can lead to greater overlap between the covariances of adjacent Gaussian components, which degrades the ability to represent the unknown PDF. This is a common issue and Psiaki [16], [17] proposed the MI bounding to set the upper limit of the covariance of each Gaussian component. The proposed filter is equipped with the MI bounding and this limits the expansion of covariance of the Gaussian component over the limit and ensures the GMM is closer to the unknown distribution we are trying to approximate using GMM. Furthermore, the proposed filter utilizes the concept of scaled sample covariance and this characteristic differentiates the proposed filter from other GMFs such as [17].

A comparison of PF, PGM filters and the proposed GMF filter approaches is shown in Table I and the graphical illustration of different ways of PDF approximation of these approaches are shown in Fig. 2.

A. Initialization

The filter is initialized with N_p samples drawn from the Gaussian distribution and the covariance of each Gaussian component is initialized as follows:

$$\mathbf{x}_0^i \sim \mathcal{N}(\boldsymbol{\mu}_0, \mathbf{P}_0), \quad i = 1, \dots, N_p, \quad (4)$$

$$\mathbf{P}_0^i = h^2 \mathbf{I}_{n \times n}, \quad (5)$$

where $h = N_p^{-0.2}$ is the bandwidth parameter with the exponent -0.2 (or $-1/5$) that is a commonly used rule of thumb to balance the trade-off between bias and variance in kernel density estimation [18], [19]. This bandwidth parameter determines the relative width of the covariance based on the number of samples, N_p , to minimize the overlap between each Gaussian component.

B. Time Propagation

Mean and covariance estimates in Eqs. (4) and (5) of each Gaussian component are propagated independently with dynamics $f(\cdot)$ and the Jacobian of dynamics in given time step k , \mathbf{F}_k^i as follows:

$$\mathbf{x}_{k|k-1}^i = f(\mathbf{x}_{k-1}^i, \mathbf{w}_k), \quad (6)$$

$$\mathbf{P}_{k|k-1}^i = \mathbf{F}_k^i \mathbf{P}_{k-1}^i \mathbf{F}_k^{iT} + \boldsymbol{\Gamma}_k \mathbf{Q}_k \boldsymbol{\Gamma}_k^T, \quad (7)$$

where $\mathbf{w}_k \sim \mathcal{N}(0, \mathbf{Q}_k)$ is a zero-mean Gaussian process noise with covariance \mathbf{Q}_k and $\boldsymbol{\Gamma}_k$ is a process noise model. To prevent the overlap between Gaussian components from becoming too large, we adopt the idea of substituting the covariance if the covariance is bigger than the upper limit of covariance with scaled sample covariance as follows:

$$\mathbf{P}_{k|k-1}^{\text{scaled}} = h^2 \frac{1}{N_p - 1} \sum_{i=1}^{N_p} (\mathbf{x}_{k|k-1}^i - \bar{\mathbf{x}}_k)(\mathbf{x}_{k|k-1}^i - \bar{\mathbf{x}}_k)^T, \quad (8)$$

where the sample covariance of the samples is scaled down with bandwidth parameter h to ensure that the covariance does not become overly large while calculating the covariance adaptively. It is worth noting that, in this study, the scaled sample covariance is introduced to replace the the predefined covariance in the MI bounding step which is the distinct point from the original idea in [16], [17].

C. Measurement Update

Each Gaussian component with time propagated mean and covariance (or scaled sample covariance) is updated with measurement from the sensor and the process of measurement update is the same as an EKF. The additional calculation of the weight w^i of each Gaussian component, using the Gaussian likelihood update (as in PF) is required to reconstruct the GMM. These processes are shown as follows:

$$\mathbf{S}_k^i = \mathbf{H}_k^i \mathbf{P}_{k|k-1}^i \mathbf{H}_k^{iT} + \mathbf{R}_k, \quad (9)$$

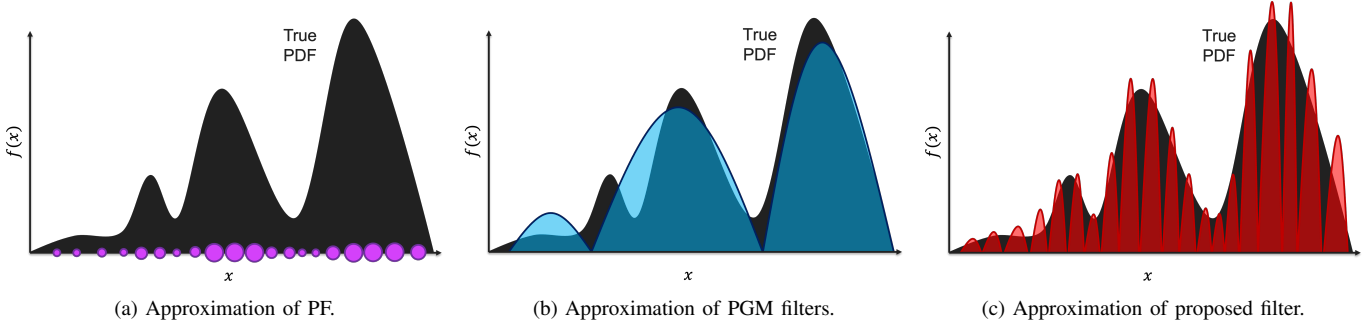


Fig. 2: **A graphical conceptualization of the PDF approximation by different approaches.** PF, PGM filters, and the proposed filter. PFs use particles and the weight of each particle, PGM filters cluster the particles and construct the GMM PDF using clusters, and GMF considers every sample as a Gaussian distribution.

$$\mathbf{K}_k^i = \mathbf{P}_{k|k-1}^i \mathbf{H}_k^{iT} (\mathbf{S}_k^i)^{-1}, \quad (10)$$

$$w_k^i = w_{k-1}^i \cdot \frac{e^{-(\mathbf{z}_k - \mathbf{H}_k^i \mathbf{x}_{k|k-1}^i)^2 / 2\sigma}}{\sqrt{2\pi R_k}}, \quad (11)$$

$$\mathbf{x}_k^i = \mathbf{x}_{k|k-1}^i + \mathbf{K}_k^i (\mathbf{z}_k - \mathbf{H}_k^i \mathbf{x}_{k|k-1}^i), \quad (12)$$

$$\mathbf{P}_k^i = (\mathbf{I} - \mathbf{K}_k^i \mathbf{H}_k^i) \mathbf{P}_{k|k-1}^i, \quad (13)$$

where \mathbf{S}_k^i is the innovation covariance with measurement noise covariance \mathbf{R}_k , \mathbf{K}_k^i is the Kalman gain for the i^{th} sample and \mathbf{z}_k is the measurement at k^{th} time step.

D. Resampling

The samples are then resampled from the GMM after the measurement update as follows:

$$\mathbf{x}_k^i \sim \sum_{i=1}^{N_p} w_k^i \mathcal{N}(\mathbf{x}_k^i, \mathbf{P}_k^i). \quad (14)$$

Also, the covariance of each resampled sample is reset with the scaled sample covariance of Eq. 8. This step prevents the sample degeneracy issue and ensures the covariance of each Gaussian component is small enough to represent the posterior distribution precisely.

IV. NUMERICAL SIMULATION RESULTS AND ANALYSIS: BLIND TRICYCLIST PROBLEM

The blind tricyclist problem [20] is a benchmark example for the nonlinear filters proposed by Psiaki. This problem considers a tricyclist navigating around a park based only on measurements of the two relative bearings where these measurements are intermittent. This problem is highly nonlinear with low observability. The 7-dimensional state vector,

$$\mathbf{x} = [X, Y, \theta, \dot{\phi}_1, \dot{\phi}_2, \dot{\phi}_3]^T, \quad (15)$$

represents the position and heading of the tricyclist, as well as the initial angles and angular velocities of two friends on a merry-go-round. The 2-dimensional measurement vector,

$$\mathbf{y} = [\psi_1, \psi_2]^T, \quad (16)$$

consists of the relative bearings between the tricyclist and the two friends, respectively. This example was adopted for many nonlinear filters and is used here to validate the performance of the proposed filter and the implementations of the compared filters. Further details of the problem can be found in [20].

The proposed filter is compared with the state-of-the-practice PF and PGM filters, as other filters were evaluated in previous studies. All filters were utilized with 7,000 samples, the process noise covariance $Q = \text{diag}([0.0567, 0.0000, 0.0063, 0.0063, 0.0000])$ and the measurement noise covariance $R = 10^{-3} [0.3046 \ 0 \ 0 \ 0.1354]$. The initial state for each Monte Carlo (MC) simulation is selected with an initial covariance matrix $P_0 = \text{diag}([18.75^2, 18.75^2, (5\pi/8)^2, (5\pi/6)^2, (5\pi/6)^2, (1.857 \times 10^{-2})^2, (1.857 \times 10^{-2})^2])$. The bandwidth parameter h of the proposed filter, the radius ϵ and the minimum points minPts used for clustering in DBSCAN for PGM filters, and the UT parameters for PGM-DU filter are shown in Table II.

TABLE II: Parameters of the tested filters for the blind tricyclist benchmark problem.

Algorithm	Module	Parameter	Value
Proposed	DBSCAN	h	$N_p^{-0.2}$
		ϵ	5.0
		minPts	8
		α	0.01
PGM-DU	UT	β	2
		κ	0

In order to compare the performance of the proposed filter with other filters, Root Mean Square Error (RMSE) of terminated position, average RMSE throughout the simulation time (ARMSE) and average simulation time are considered as performance metrics. Average simulation time here refers to the required time to run one MC simulation. A total

number of 100 MC simulations is conducted and the results are shown in Table III.

TABLE III: Results of blind tricyclist problem.

Algorithm	Terminate RMSE (m)	Position ARMSE (m)	Average simulation time (sec)
Proposed	5.6348	13.8535	113.0153
PGM-DS	119.6745	101.8103	236.0642
PGM-DU	10.2320	22.6147	254.1003
PF	11.9186	26.1625	49.5318

The results show that the proposed filter performs better than compared filters in terms of estimation error: terminate RMSE and ARMSE. Also, the proposed filter can reduce the estimation time by half compared to PGM filters. The convergence of RMSE of the simulation example is shown in Fig. 3.

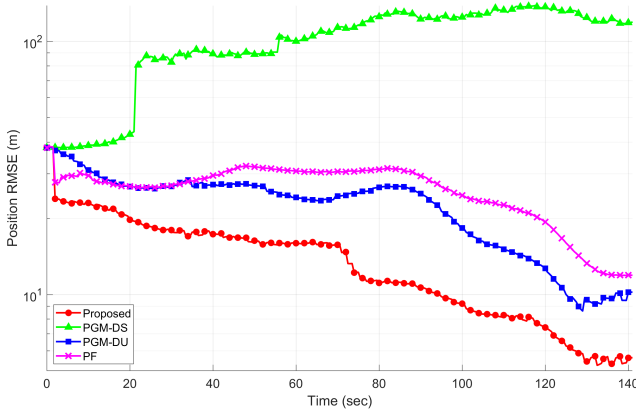


Fig. 3: **Results of blind tricyclist problem.** The proposed filter showed the faster convergence over other compared filter with smaller terminate RMSE and ARMSE.

V. EXPERIMENTAL RESULTS FOR AN AUTONOMOUS ROBOTIC RADIO SIGNAL SOURCE SEARCH AND LOCALIZATION MISSION

A. Overview

For demonstration towards real-world applications, the scenario for an autonomous multi-robot search and localization of multiple radio signal sources in an unknown environment is considered. In this study, we considered scenarios in which two legged robots (Boston Dynamics Spot), equipped with custom compute and sensing payloads [21], attempt to localize two radio signal source simultaneously but independently. Each robot autonomously explores the unknown environment and localizes its tasked radio signal source independently, without utilizing any prior information. Fig. 4 shows the experiment setup presentation the mission environment map (shown for illustration here), the allowed exploration area marked with white boundary, the starting location of the two robots marked in yellow, and the unknown locations of the two radio sources marked in red.

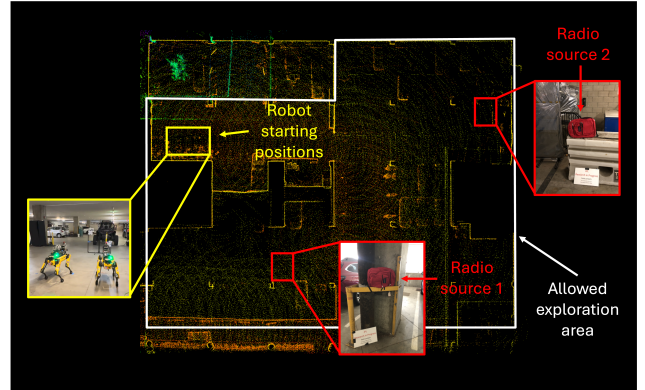


Fig. 4: **Example test environment.** The yellow box indicates the starting positions of the robots, while the two red boxes mark the locations of the radio signal sources. The white box represents the allowed exploration area.

This study is focused on the estimation of the position of the radio signal sources and the exploration methodology and Simultaneously Localization and Mapping (SLAM) techniques fall outside of this study's scope. Further detail for autonomous exploration [22] and SLAM [23] are available in previous studies.

B. Measurement Model

Radios operating in the 5 GHz range are utilized as a signal sources to localize. Two radios are placed in an unknown space with their signal being measured by the two robots. Only the Signal-to-Noise Ratio (SNR) value is measured by the robots as an indicator radio signal strength with respect to distance from the robots. In other words, no direct manner of measuring the distance or bearing between the robot and the signal source. Furthermore, the SNR value is a noisy indicator of radio distance from the robot as LOS and Non-LOS (NLOS) SNR measurements can result in the same value while at different distances from the robot. A bimodal log-linear measurement model is considered to predict signal strength given the distance between the position of the robot and the estimated sample radio location, d_i . The predicted signal strength for the i^{th} sample, z_k^i can be calculated with two tuning parameters, log-linear multiplier p_1 and log-linear constant p_2 as follows:

$$z_k^i = p_1 \log_{10}(d_i) + p_2. \quad (17)$$

The term “bimodal” here refers to the consideration of the probability that the signal source being on either the LOS and NLOS at each measurement step. The predicted signal strength in Eq. 17 is calculated twice: once for the LOS case and once for the NLOS case, each with different parameters p_1 and p_2 . To determine the probability of being on LOS or NLOS, the filter first check if the sample is within a threshold distance from the position of the robot. Then, if the sample is within the threshold distance, the probability of the sample being on the LOS is set to 0.95, while on the NLOS is set

to 0.05. On the other hand, if the sample is not within the threshold distance, the probability of the sample being LOS is set to 0.5 and on the NLOS to 0.5. Finally, the weight of each sample is computed as a linear combination of the LOS and NLOS cases, weighted by their respective probabilities. It is worth noting that given a measurement that can be interpreted as a range-only without bearing information, and the robot's current position, the belief of the state can be ring-shaped.

C. Evaluation Metrics

In order to evaluate and compare the tested filters, two evaluation metrics are considered. The average position error estimation is the first metric to evaluate the estimation accuracy of the filters throughout the test time. It is calculated by time-averaging the distance between the estimated mean and the true position of the radio signal source. This metric is chosen to show the accuracy of the proposed and compared filters. The second metric is the average iteration time, which is used to evaluate the computation cost of the presented methods. This metric is important to ensure that the proposed and compared methods are suitable for real-time online applications towards real-world robotic applications. The average iteration time is calculated by averaging the time elapsed during each iteration of the filter throughout the experiment. In addition, the average number of Gaussian components is presented for a monitoring purpose. This is to monitor how many clusters are considered to construct the GMM for the proposed filter and PGM filters. Note that the proposed filter considers all samples as individual Gaussian distributions and the number of components remains constant.

D. Experimental Results and Discussion

The proposed filter was tested with real-world data of the considered scenarios as described in Section V and compared against the performance of two PGM filters, PGM-DS and PGM-DU filters and PF. All filters were utilized with 3,000 samples, the process noise covariance $Q = 0.5$ and the measurement noise covariance as a linear combination of $R_{min} = 8$ and $R_{max} = 35$ based on the SNR. This adaptive measurement noise covariance allows the filter to adjust dynamically based on the SNR, making it trust the measurements more as it gets closer to the source with a higher SNR. The bandwidth parameter h of the proposed filter, the radius ϵ and the minimum points $minPts$ used for clustering in DBSCAN for PGM filters, and the UT parameters for PGM-DU filter are shown in Table IV.

TABLE IV: Parameters of the tested filters for the autonomous robotic radio signal source search and localization mission.

Algorithm	Module	Parameter	Value
Proposed	-	h	$N_p^{-0.2}$
PGM Filters	DBSCAN	ϵ	1.0
		$minPts$	4
		α	0.001
PGM-DU	UT	β	2
		κ	0

Two experiments were conducted to evaluate the performance of all methods. In the first experiment, the radio signal sources were placed in the direct LOS of the robot to mitigate any effects of radio signal reflection from the environment. In the second experiment, the radio signal sources were placed outside the direct LOS of the robot and hidden closer corners in the unknown environment. Each experimental scenario contained two radio signal sources to be searched for and localized by the two robots. Note that each robot localizes each target independently as already mentioned in Section V. The test results of the search and localization and standard deviations for the two experimental scenarios are presented in Tables V and VI, as well as Fig. 5.

TABLE V: Results of scenario 1.

Algorithm	Average position estimation error (m)	Average iteration time (sec)	Average number of components
Proposed	19.0	0.22	3000
PGM-DS	18.8	0.80	30.6
PGM-DU	21.9	0.71	4.9
PF	20.9	0.08	-

TABLE VI: Results of scenario 2.

Algorithm	Average position estimation error (m)	Average iteration time (sec)	Average number of components
Proposed	16.9	0.22	3000
PGM-DS	22.4	0.73	19.0
PGM-DU	40.8	0.72	21.5
PF	26.7	0.08	-

In the first scenario, the proposed filter showed an average position estimation error of 19.0 m whilst the other filters, PGM-DS, PGM-DU and PF showed 18.8 m, 21.9 m and 20.9 m, respectively. Moreover, the average iteration time of the proposed filter was 0.22 seconds whilst the other filters were 0.80 seconds, 0.71 seconds and 0.08 seconds, respectively. In the second scenario, the proposed filter showed an average position estimation error of 16.9 m whilst the other filters, PGM-DS, PGM-DU and PF showed 22.4 m, 40.8 m and 26.7 m, respectively. Moreover, the average iteration time of the proposed filter was 0.22 seconds whilst the other filters were 0.73 seconds, 0.72 seconds and 0.08 seconds, respectively. It is worth noting that the proposed filter and PF were able to estimate the belief with a ring shape, whereas the PGM filters were not able to do so, as expected. A summary of the performance of each filter on average from both scenarios and the tested scenarios is shown in Fig. 6.

The test results of the first scenario, where the radio signal sources were located on the LOS of the robots, showed that the proposed filter performs the second-best in average position estimation error of 19.0 m whereas PGM-DS showed the smallest error of 18.8 m. Although the average position error of the proposed filter was larger than PGM-DS, the proposed filter

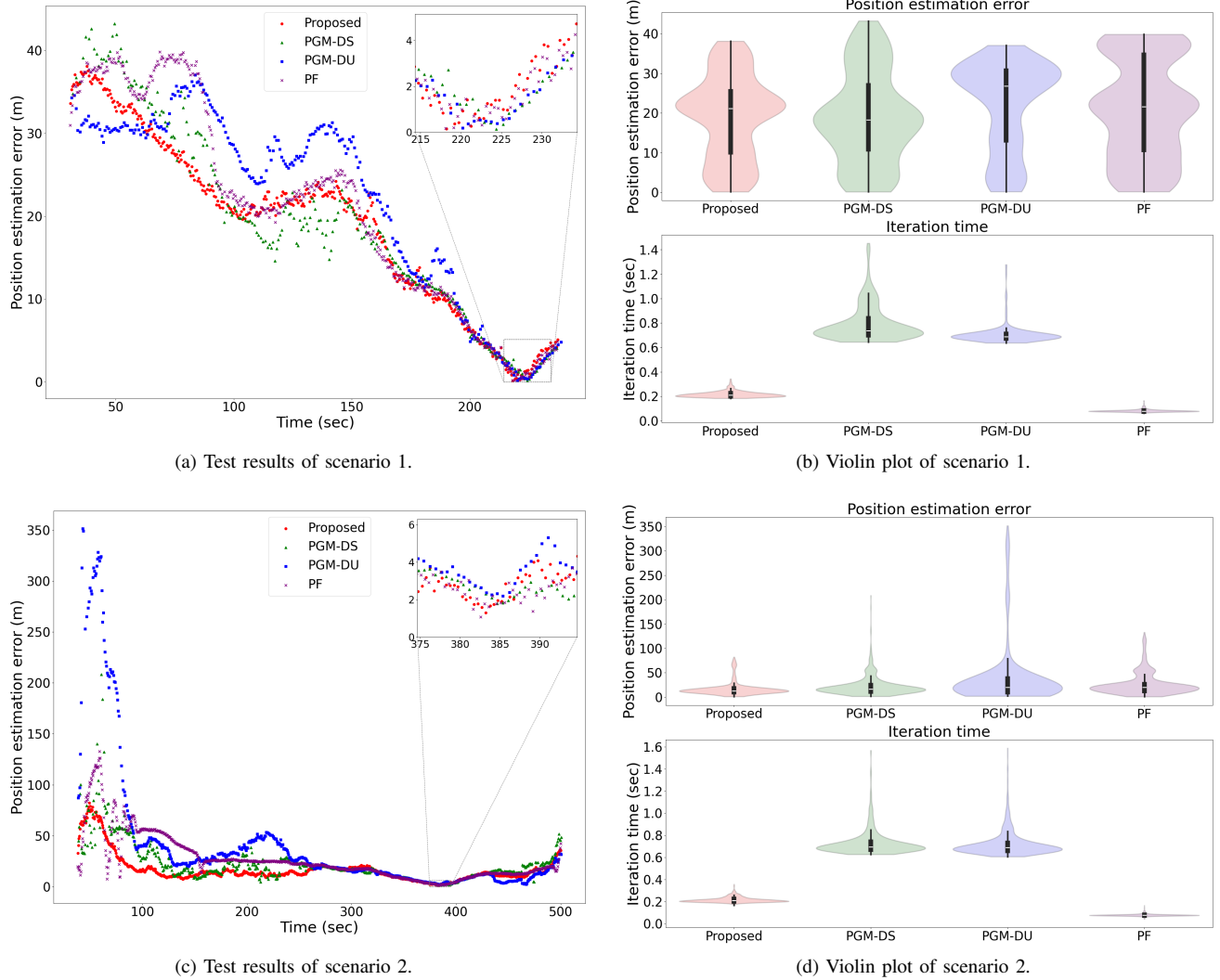


Fig. 5: Evaluation of the proposed approach against benchmarks (PGM-DS, PGM-DU, and PF) regarding i) position estimation error profiles over operational time and ii) statistical distributions in position estimation errors and iteration times. Note that sub-figures (a) and (c) correspond to Scenario 1 and other sub-figures (b) and (d) related to Scenario 2.

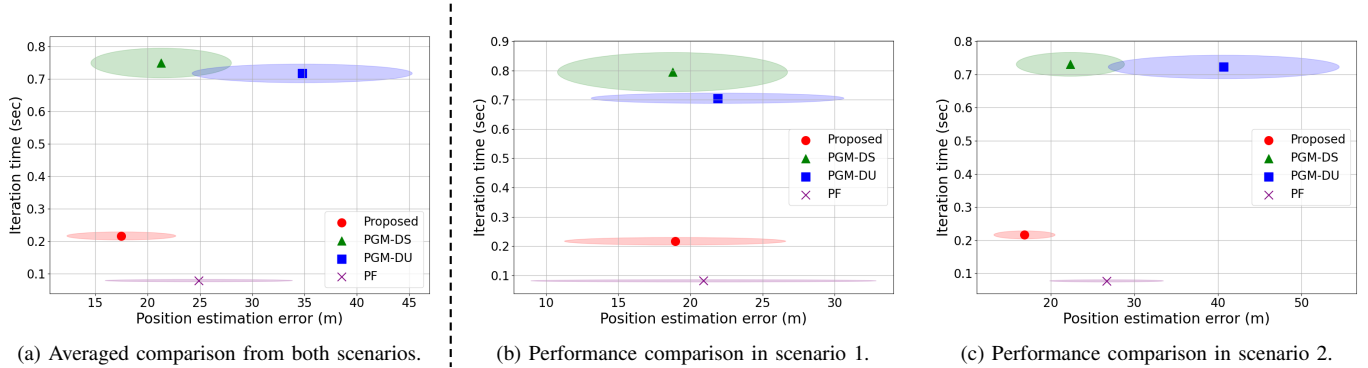


Fig. 6: The visualized comparison in terms of position estimation error (x-axis) and iteration time (y-axis). (a) shows the averaged results from both two scenarios, whilst (b) and (c) are results from Scenario 1 and Scenario 2 respectively. Note that markers and ovals represent mean and region within 2- σ bounds in distribution respectively.

was 3.64 times faster than PGM-DS. In the second scenario, where the radio signal sources were located outside the LOS of the robots, the proposed filter showed the smallest average position estimation error of 16.9 m which is 24.6% improvement from the second-best performance, 22.4 m of PGM-DS. In this case, the proposed filter was again 3.32 times faster than PGM-DS. Throughout the scenarios, PF was the fastest and the proposed filter was the second fastest whilst PGM-DS and PGM-DU were approximately three times slower than the proposed filter. It is worth mentioning that the average iteration time of each tested filter was less than one second. This indicates that all filters can be utilized in online estimation applications with a 1 Hz update, which is the case of the tested environment.

In addition to the improved performance with less computation than PGM filters, the proposed filter showed smaller deviation in both position error and iteration time as is shown in Fig. 5 (b) and (d). In the first scenario, PGM-DU and PF showed high occurrence in the high error region whilst the proposed filter and PGM-DS filter showed high occurrence around the mean. In the second scenario, the proposed filter showed the smallest deviation of position estimation error whilst the other filters showed larger deviation with larger maxima. In the case of iteration time, the proposed filter showed a much smaller deviation compared to PGM filters as shown in Fig. 5 (b) and (d). This indicates that the proposed filter shows consistency of good performance and robustness throughout the tested scenarios.

VI. CONCLUSION

A new GMF was proposed with the addition of MI bounding and scaled sample covariance for resampling. The proposed filter was tested in a numerical benchmark problem and showed enhanced performance over PF and PGM filters. Moreover, the proposed filter was tested in the two autonomous robotic radio signal source search scenarios with partial observability and compared with PF and PGM filters. The results showed the efficiency and versatility of the proposed method over other filters in the partially observable scenario. Also, the experimental results showed that the proposed filter can be applied to the online radio signal source search scenario with robust estimation. However, the tested scenarios consider only one measurement from one robot whilst multiple measurements can be considered to improve the observability. Constructing the joint belief using a data fusion approach with multiple measurements from multiple robots to improve estimation performance remains as future work. Additionally, introducing hypothesis reduction and component merging can also reduce computation and is considered as future work.

REFERENCES

- [1] C. E. Denniston, O. Peltzer, J. Ott, S. Moon, S.-K. Kim, G. S. Sukhatme, M. J. Kochenderfer, M. Schwager, and A.-a. Agha-mohammadi, "Fast and scalable signal inference for active robotic source seeking," in 2023 *IEEE International Conference on Robotics and Automation (ICRA)*, 2023, pp. 7909–7915.
- [2] S.-i. Azuma, M. S. Sakar, and G. J. Pappas, "Stochastic source seeking by mobile robots," *IEEE Transactions on Automatic Control*, vol. 57, no. 9, pp. 2308–2321, 2012.
- [3] S. Li, R. Kong, and Y. Guo, "Cooperative distributed source seeking by multiple robots: Algorithms and experiments," *IEEE/ASME Transactions on Mechatronics*, vol. 19, no. 6, pp. 1810–1820, 2014.
- [4] A. Turgeman and H. Werner, "Multiple source seeking using glowworm swarm optimization and distributed gradient estimation," in 2018 *Annual American Control Conference (ACC)*, 2018, pp. 3558–3563.
- [5] A. Agha, K. Otsu, B. Morrell, D. D. Fan, R. Thakker, A. Santamaría-Navarro, S.-K. Kim, A. Bouman, X. Lei, J. Edlund *et al.*, "Nebula: Quest for robotic autonomy in challenging environments; team costar at the darpa subterranean challenge," *arXiv preprint arXiv:2103.11470*, 2021.
- [6] M. Park and H. Oh, "Cooperative information-driven source search and estimation for multiple agents," *Information Fusion*, vol. 54, pp. 72–84, 2020.
- [7] L. Clark, J. A. Edlund, M. S. Net, T. S. Vaquero, and A.-a. Agha-Mohammadi, "Propem-l: Radio propagation environment modeling and learning for communication-aware multi-robot exploration," *arXiv preprint arXiv:2205.01267*, 2022.
- [8] N. J. Gordon, D. J. Salmond, and A. F. M. Smith, "Novel approach to nonlinear/non-Gaussian Bayesian state estimation," *IEE Proceedings F Radar and Signal Processing*, vol. 140, no. 2, p. 107, 1993.
- [9] P. M. Djuric, J. H. Kotecha, J. Zhang, Y. Huang, T. Ghirmai, M. F. Bugallo, and J. Miguez, "Particle Filtering," *IEEE Signal Processing Magazine*, vol. 20, no. 5, pp. 19–38, 2003.
- [10] J. Candy, "Bootstrap Particle Filtering," *IEEE Signal Processing Magazine*, vol. 24, no. 4, pp. 73–85, 2007.
- [11] T. Li, S. Sun, T. P. Sattar, and J. M. Corchado, "Fight sample degeneracy and impoverishment in particle filters: A review of intelligent approaches," *Expert Systems with Applications*, vol. 41, no. 8, pp. 3944–3954, 2014.
- [12] D. Alspach and H. Sorenson, "Nonlinear bayesian estimation using gaussian sum approximations," *IEEE transactions on automatic control*, vol. 17, no. 4, pp. 439–448, 2003.
- [13] D. Raihan and S. Chakravorty, "Particle Gaussian mixture filters-I," *Automatica*, vol. 98, pp. 331–340, 2018.
- [14] ———, "Particle Gaussian mixture filters-II," *Automatica*, vol. 98, pp. 341–349, 2018.
- [15] S. Kim, M. Sun, H.-S. Shin, and I. Petrunin, "DBSCAN-based particle Gaussian mixture filters," Available at SSRN 5158079.
- [16] M. L. Psiaki, J. R. Schoenberg, and I. T. Miller, "Gaussian Sum Reapproximation for Use in a Nonlinear Filter," *Journal of Guidance, Control, and Dynamics*, vol. 38, no. 2, pp. 292–303, 2015.
- [17] M. L. Psiaki, "Gaussian Mixture Nonlinear Filtering With Resampling for Mixand Narrowing," *IEEE Transactions on Signal Processing*, vol. 64, no. 21, pp. 5499–5512, 2015.
- [18] B. W. Silverman, *Density estimation for statistics and data analysis*. Routledge, 2018.
- [19] A. S. Stordal, H. A. Karlsen, G. Nævdal, H. J. Skaug, and B. Vallès, "Bridging the ensemble kalman filter and particle filters: the adaptive gaussian mixture filter," *Computational Geosciences*, vol. 15, pp. 293–305, 2011.
- [20] M. Psiaki, "The blind tricyclist problem and a comparative study of nonlinear filters: A challenging benchmark for evaluating nonlinear estimation methods," *IEEE Control Systems*, vol. 33, no. 3, pp. 40–54, 2013.
- [21] A. Bouman, M. F. Ginting, N. Alatur, M. Palieri, D. D. Fan, T. Touma, T. Paileyanian, S.-K. Kim, K. Otsu, J. Burdick, and A.-a. Agha-Mohammadi, "Autonomous spot: Long-range autonomous exploration of extreme environments with legged locomotion," in 2020 *IEEE/RSJ International Conference on Intelligent Robots and Systems (IROS)*, 2020, pp. 2518–2525.
- [22] S. Moon, S.-K. Kim, O. Peltzer, M. J. Kochenderfer, and S. Khattak, "Efficient line-of-sight viewpoint sampling in complex environments for autonomous surface inspection," in 2024 *IEEE International Symposium on Safety Security Rescue Robotics (SSRR)*. IEEE, 2024, pp. 198–203.
- [23] S. Fakoorian, K. Otsu, S. Khattak, M. Palieri, and A.-a. Agha-mohammadi, "Rose: Robust state estimation via online covariance adaptation," in *The International Symposium of Robotics Research*. Springer, 2022, pp. 452–467.